EUROPEAN ORGANIZATION FOR NUCLEAR RESEARCH

CERN-PH-EP/2004-016
April 22, 2004

Search for Branons at LEP

The L3 Collaboration

Abstract

We search, in the context of extra-dimension scenarios, for the possible existence of brane fluctuations, called *branons*. Events with a single photon or a single Z-boson and missing energy and momentum collected with the L3 detector in e^+e^- collisions at centre-of-mass energies $\sqrt{s} = 189 - 209$ GeV are analysed. No excess over the Standard Model expectations is found and a lower limit at 95% confidence level of 103 GeV is derived for the mass of branons, for a scenario with small brane tensions. Alternatively, under the assumption of a light branon, brane tensions below 180 GeV are excluded.

Submitted to *Phys. Lett. B*

1 Introduction

The possible existence of additional space dimensions was suggested by Kaluza and Klein [1] more than eighty years ago. In the original theory, the fundamental scale of gravitation, M_F, coincides with the Planck scale, $M_P \approx 10^{19}$ GeV. Since then, several theories have used this idea as an alternative way to solve some fundamental problems of physics, particularly those related with gravitation and the unification of all forces. One of the most attractive models is proposed in Reference 2. This model assumes the restriction of the dynamics of the Standard Model to a three-dimensional spatial brane, leaving the gravitation and perhaps some other exotic particles the freedom to propagate in the extra dimensions. If these extra dimensions have a large size, M_F is of the order of the electroweak scale and the existence of extra dimensions could manifest at present and future colliders with detection of gravitons, as described by an effective theory with couplings of order M_F.

A different scenario is considered in this Letter. In this approach, the presence of a three-dimensional brane as an additional physical body in the theory, with its own dynamics, leads to the appearance of additional degrees of freedom. These manifest as new scalar particles, $\tilde{\pi}$, called *branons*. Branons are associated to brane fluctuations along the extra-dimensions [3] and are also natural dark-matter candidates [4]. Their dynamics is determined by an effective theory with couplings of the same order as the brane tension, f.

Searches for gravitons and branons are in a sense complementary [5]. If the brane tension is above the gravity scale, $f \gg M_F$, the first evidence for extra dimensions would be the discovery of gravitons, giving information about the fundamental scale of gravitation and the characteristics of the extra dimensions. If the brane tension is below the gravity scale, $f \ll M_F$, then the first signal of extra dimensions would be the discovery of branons, allowing a measurement of the brane tension scale, the number of branons and their masses [6].

Many experimental results were reported on direct searches for gravitons at LEP [7–9] and at the TEVATRON [10]. This Letter describes a search for branons in data collected at LEP. Branons couple to Standard Model particles by pairs, suggesting the study of two production mechanisms in $\mathrm{e^+e^-}$ collisions: $\mathrm{e^+e^-} \to \tilde{\pi}\tilde{\pi}\gamma$ and $\mathrm{e^+e^-} \to \tilde{\pi}\tilde{\pi}\mathrm{Z}$. They proceed via the diagrams shown in Figure 1. The experimental signature for branon production at LEP is the presence of either a photon or a Z boson together with missing energy and momentum. This is due to the two branons which do not interact in the detector and are hence invisible. In the following, only decays of the Z boson into hadrons are considered. For a given centre-of-mass energy, only the lighter branons give a significant contribution to the cross sections of the $\mathrm{e^+e^-} \to \tilde{\pi}\tilde{\pi}\gamma$ and $\mathrm{e^+e^-} \to \tilde{\pi}\tilde{\pi}\mathrm{Z}$ processes. For simplicity, we will assume a scenario with only one light branon species of mass M.

2 Data and Monte Carlo Samples

Data collected by the L3 detector [11] at LEP in the years from 1998 through 2000 are considered. They correspond to an integrated luminosity of about 0.6 fb^{-1} at centre-of-mass energies, $\sqrt{s}$, from 188.6 to 209.2 GeV.

The following Monte Carlo generators are used to simulate Standard Model processes: `KK2f` [12] for $\mathrm{e^+e^-} \to \nu\bar{\nu}\gamma(\gamma)$ and $\mathrm{e^+e^-} \to \mathrm{q\bar{q}}(\gamma)$, `GGG` [13] for $\mathrm{e^+e^-} \to \gamma\gamma(\gamma)$, `BHWIDE` [14] and `TEEGG` [15] for large- and small-angle Bhabha scattering, respectively, `PHOJET` [16] and `DIAG36` [17] for hadron and lepton production in two-photon interactions, `KORALW` [18] for W-boson pair-production and `EXCALIBUR` [19] for Z-boson pair-production and other four-fermion final states. The predictions of KK2f for the $\mathrm{e^+e^-} \rightarrow \nu\bar{\nu}\gamma(\gamma)$ process are checked with the NUNUGPV [20] generator.

The efficiencies for branon production through the processes $\mathrm{e^+e^-} \rightarrow \tilde{\pi}\tilde{\pi}\gamma$ and $\mathrm{e^+e^-} \rightarrow \tilde{\pi}\tilde{\pi}\mathrm{Z} \rightarrow \tilde{\pi}\tilde{\pi}\mathrm{q\bar{q}}$ are determined by reweighting Monte Carlo events of the processes $\mathrm{e^+e^-} \rightarrow \nu\bar{\nu}\gamma(\gamma)$ and $\mathrm{e^+e^-} \rightarrow \nu\bar{\nu}\mathrm{Z} \rightarrow \nu\bar{\nu}\mathrm{q\bar{q}}$, respectively, with the differential cross sections of Reference 6. Events from the first process are generated with KK2f and events from the second process with EXCALIBUR, through W-boson fusion.

The L3 detector response is simulated using the GEANT program [21], which describes effects of energy loss, multiple scattering and showering in the detector. Time-dependent detector inefficiencies, as monitored during the data-taking period, are included in the simulation.

3 Search in the $\mathrm{e^+e^-} \rightarrow \tilde{\pi}\tilde{\pi}\mathrm{Z} \rightarrow \tilde{\pi}\tilde{\pi}\mathrm{q\bar{q}}$ channel

The single-Z signature for branon production at LEP is similar to the signature of the associated production of a Z boson and a graviton which was previously studied in data collected by L3 at $\sqrt{s} = 188.6$ GeV [8]. The events selected for that search are re-analysed in this Letter to search for branons, and the same analysis procedure is used to select candidate events at $\sqrt{s} = 191.6 - 209.2$ GeV. The integrated luminosities considered for each value of $\sqrt{s}$ are listed in Table 1.

Unbalanced hadronic events with a visible mass compatible with that of the Z boson are selected. The large background from $\mathrm{e^+e^-} \rightarrow \mathrm{q\bar{q}}\gamma$ events with a low-angle high-energy photon is reduced by requiring the missing momentum vector to point in the detector. Cuts on event-shape and jet-shape variables are applied to suppress other backgrounds: Z-boson pair-production with one of the Z bosons decaying into neutrinos and the other into hadrons, W-boson pair-production with one of the W bosons decaying into hadrons and the other into a low-angle undetected charged lepton and a neutrino, and single-W production through the $\mathrm{e^+e^-} \rightarrow \mathrm{We}\nu$ process, followed by a hadronic decay of the W boson.

Table 1 summarises the yield of the selection at the different centre-of-mass energies. In total, 455 events are observed while 470 events are expected from several Standard Model processes. The dominant background is W-boson pair-production (47%). Other sources of background are single-W production (25%), Z-boson pair-production (13%) and the $\mathrm{e^+e^-} \rightarrow \mathrm{q\bar{q}}\gamma$ process (12%).

Expectations for a branon signal with $M = 0$ and $f = 40$ GeV are also listed in Table 1. The efficiency to detect such a signal is 55%. Two variables are most sensitive to discriminate a possible signal from the Standard Model background: the reduced energy of the Z boson, $x_\mathrm{Z} = E_\mathrm{Z}/\sqrt{s}$, and the cosine of its polar angle, $\cos\theta_\mathrm{Z}$. The distribution of these variables for data and Standard Model backgrounds are shown in Figures 2a and 2b. These Figures also show the predictions in the presence of a branon signal. No excess with respect to the Standard Model expectations is observed.

4 Search in the $\mathrm{e^+e^-} \rightarrow \tilde{\pi}\tilde{\pi}\gamma$ channel

Events with a single photon and large missing energy and momentum, selected by L3 at $\sqrt{s} = 188.6 - 209.2$ GeV [7], are re-analysed for the presence of a signal due to the $\mathrm{e^+e^-} \rightarrow \tilde{\pi}\tilde{\pi}\gamma$ process in addition to the Standard Model contributions from the $\mathrm{e^+e^-} \rightarrow \nu\bar{\nu}\gamma(\gamma)$ and $\mathrm{e^+e^-} \rightarrow \mathrm{e^+e^-}\gamma(\gamma)$ processes. A breakdown of the integrated luminosities as a function of $\sqrt{s}$ is given in

Table 2. Two different energy regimes are considered, depending on the value of the transverse momentum of the photon, p_t, relative to the beam energy, E_{beam}, and its polar angle, θ_γ. High-p_t events, $0.04E_{beam} < p_t < 0.60E_{beam}$, are selected in both the barrel, $|\cos\theta_\gamma| < 0.73$, and endcap, $0.8 < |\cos\theta_\gamma| < 0.97$, regions of the electromagnetic calorimeter. The selection of low-p_t events, $0.016E_{beam} < p_t < 0.04E_{beam}$, relies on a single-photon energy trigger with a threshold around 900 MeV which is active only in the barrel region [22].

Table 2 lists the number of observed data events together with the Standard Model expectations for different values of $\sqrt{s}$. The high-p_t analysis selects $\mathrm{e^+e^-} \to \nu\bar{\nu}\gamma(\gamma)$ events with purity above 99% and efficiency above 80%. In total, 838 events are observed in data while 811 are expected from Standard Model processes. Figures 3a and 3b show the measured differential cross sections for the $\mathrm{e^+e^-} \to \nu\bar{\nu}\gamma(\gamma)$ processes as a function of $x_\gamma = E_\gamma/E_{beam}$, the fraction of the beam energy carried by the photon and of $|\cos\theta_\gamma|$. Data obtained by the high-p_t selection are corrected for detector acceptance and integrated over the polar-angle fiducial region $|\cos\theta_\gamma| < 0.97$. The measured differential cross sections are in good agreement with the Standard Model expectations.

The criteria of the low-p_t selections are much more stringent in order to be sensitive to very low photon energies while minimizing the huge $\mathrm{e^+e^-} \to \mathrm{e^+e^-}\gamma(\gamma)$ component. In total, 543 events are observed in data and 554 are expected from Standard Model processes. The main contribution is from $\mathrm{e^+e^-} \to \mathrm{e^+e^-}\gamma(\gamma)$ events and the $\mathrm{e^+e^-} \to \nu\bar{\nu}\gamma(\gamma)$ purity is around 24%. The event selection is described in detail in Reference 7. Figures 4a and 4b compare the distributions of x_γ and $|\cos\theta_\gamma|$ observed in data with the expectations of the Standard Model processes. A good agreement is observed.

The presence of a branon leads to an increase in the differential cross sections which is a function of the branon mass M and the brane tension f [6]:

$$\begin{aligned}\frac{\mathrm{d}^2\sigma(\mathrm{e^+e^-} \to \tilde{\pi}\tilde{\pi}\gamma)}{\mathrm{d}x_\gamma \mathrm{d}\cos\theta_\gamma} &= \alpha\frac{s(s(1-x_\gamma)-4M^2)^2}{61440 f^8\pi^2}\sqrt{1-\frac{4M^2}{s(1-x)}} \\ &\quad [x_\gamma(3-3x_\gamma+2x_\gamma^2) - x_\gamma^3\sin^2\theta_\gamma + \frac{2(1-x_\gamma)(1+(1-x_\gamma)^2)}{x_\gamma\sin^2\theta_\gamma}], \qquad (1)\end{aligned}$$

where α is the electromagnetic coupling constant.

Figures 3 and 4 show the typical distortion in the differential cross sections expected in the presence of a branon signal.

5 Results

Evidence for branon production was found neither in the $\mathrm{e^+e^-} \to \tilde{\pi}\tilde{\pi}\mathrm{Z} \to \tilde{\pi}\tilde{\pi}\mathrm{q\bar{q}}$ nor in the $\mathrm{e^+e^-} \to \tilde{\pi}\tilde{\pi}\gamma$ channels and the data are interpreted in terms of bounds on the possible production of branons. For each centre-of-mass energy, the data and the expectations are compared in bins of the two-dimensional distributions of x_Z *vs.* $\cos\theta_\mathrm{Z}$ for the $\mathrm{e^+e^-} \to \tilde{\pi}\tilde{\pi}\mathrm{Z} \to \tilde{\pi}\tilde{\pi}\mathrm{q\bar{q}}$ channel and of x_γ *vs.* $\cos\theta_\gamma$ for the $\mathrm{e^+e^-} \to \tilde{\pi}\tilde{\pi}\gamma$ channel. Assuming a Poisson probability distribution for each bin, 95% confidence level exclusion limits are derived according to the method described in Reference 23. Systematic uncertainties are taken into account in the calculation of the limit. For the $\mathrm{e^+e^-} \to \tilde{\pi}\tilde{\pi}\mathrm{Z} \to \tilde{\pi}\tilde{\pi}\mathrm{q\bar{q}}$ channel, they are similar to those encountered in the study of Z-boson pair-production when one of the bosons decays into hadrons and the other into neutrinos [24] and are dominated by uncertainties on the background normalisation, on the detector energy scale and modelling and from limited Monte Carlo statistics. The main systematic uncertainties for the $e^+e^- \rightarrow \tilde{\pi}\tilde{\pi}\gamma$ channel [7] are the modelling of Standard Model process, the determination of the trigger efficiency and the treatment of photons which convert in electron-positron pairs in the detector material in front of the electromagnetic calorimeter.

The bounds from the $e^+e^- \rightarrow \tilde{\pi}\tilde{\pi}Z$ analysis are shown in Figure 5. For massless branons, the brane tension f must be greater than 47 GeV. There is no sensitivity for branon masses near and beyond the kinematic limit ($M \gtrsim (\sqrt{s} - m_Z)/2$) and no bounds on f can be derived for $M > 54$ GeV. The sensitivity in the $e^+e^- \rightarrow \tilde{\pi}\tilde{\pi}\gamma$ channel is larger than that of the $e^+e^- \rightarrow \tilde{\pi}\tilde{\pi}Z \rightarrow \tilde{\pi}\tilde{\pi}q\overline{q}$ channel. This is due to two factors: the different coupling of the Z boson and the photon to electrons and a larger phase space available in the presence of a photon in the final state, as opposed to a massive Z boson. The limits obtained from the $e^+e^- \rightarrow \tilde{\pi}\tilde{\pi}\gamma$ analysis are also shown in Figure 5. For $M = 0$, the brane tension f must be greater than 180 GeV. For very elastic branes ($f \rightarrow 0$) a lower branon mass bound of $M > 103$ GeV is obtained.

These bounds are the most stringent to date on the possible existence of branons. The bounds for $M > 0$ GeV complement and improve those deduced from astrophysical observations [4].

References

[1] T. Kaluza, Sitzungsber. Preuss. Akad. Wiss. Berlin (Math. Phys.) (1921) 966;
O. Klein, Z. Phys. **37** (1926) 895.

[2] N. Arkani-Hamed, S. Dimopoulos and G. Dvali, Phys. Lett. **B 429** (1998) 263;
N. Arkani-Hamed, S. Dimopoulos and G. Dvali, Phys. Rev. **D59**, (1999) 086004;
I. Antoniadis *et al.*, Phys. Lett. **B436** (1998) 257.

[3] R. Sundrum, Phys. Rev. **D59** (1999) 085009;
A. Dobado and A.L. Maroto, Nucl. Phys. **B 592** (2001) 203.

[4] J.A.R. Cembranos, A. Dobado and A.L. Maroto, Phys. Rev. Lett. **90** (2003) 241301;
J.A.R. Cembranos, A. Dobado and A.L. Maroto, Phys. Rev. **D68** (2003) 103505.

[5] M. Bando *et al.*, Phys. Rev. Lett. **83** (1999) 3601.

[6] J. Alcaraz *et al.*, Phys. Rev. **D67** (2003) 075010.

[7] L3 Collab., P. Achard *et al.*, Phys. Lett. **B 587** (2004) 16.

[8] L3 Collab., M. Acciarri *et al.*, Phys. Lett. **B 470** (1999) 281.

[9] ALEPH Collab., A. Heister *et al.*, Eur. Phys. J. **C 28** (2003) 1;
DELPHI Collab., P. Abreu *et al.*, Eur. Phys. J. **C 17** (2000) 53;
OPAL Collab., K. Ackerstaff *et al.*, Eur. Phys. J. **C 8** (1999) 23.

[10] D0 Collab., V.M. Abazov *et al.*, Phys. Rev. Lett. **90** (2003) 251802;
CDF Collab., D. Acosta *et al.*, preprint hep-ex/0309051 (2003);
CDF Collab., D. Acosta *et al.*, Phys. Rev. Lett. **89** (2002) 281801.

[11] L3 Collab., O. Adriani *et al.*, Phys. Rep. **236** (1993) 1;
L3 Collab., B. Adeva *et al.*, Nucl. Instr. and Meth. **A 289** (1990) 335;
M. Chemarin *et al.*, Nucl. Instr. and Meth. **A 349** (1994) 345;

M. Acciarri *et al.*, Nucl. Instr. and Meth. **A 351** (1994) 300;
G. Basti *et al.*, Nucl. Instr. and Meth. **A 374** (1996) 293;
I.C. Brock *et al.*, Nucl. Instr. and Meth. **A 381** (1996) 236;
A. Adam *et al.*, Nucl. Instr. and Meth. **A 383** (1996) 342.

[12] `KK2f` versions 4.12 and 4.19 are used for hadrons and neutrinos in the final state, respectively:
S. Jadach, B.F.L. Ward and Z. Was, Comput. Phys. Commun. **130** (2000) 260;
S. Jadach, B.F.L. Ward and Z. Was, Phys. Rev. **D 63** (2001) 113009;
D. Bardin *et al.*, Eur. Phys. J. **C 24** (2002) 373.

[13] `GGG` Monte Carlo:
F.A. Berends and R. Kleiss, Nucl. Phys. **B 186** (1981) 22.

[14] `BHWIDE` version 1.03 is used:
S. Jadach, W. Placzek and B.F.L. Ward, Phys. Lett. **B 390** (1997) 298.

[15] `TEEGG` version 7.1 is used:
D. Karlen, Nucl. Phys. **B 289** (1987) 23.

[16] `PHOJET` version 1.05c is used:
R. Engel, Z. Phys. **C 66** (1995) 203;
R. Engel and J. Ranft, Phys. Rev. **D 54** (1996) 4244.

[17] `DIAG36` Monte Carlo:
F.A. Berends, P.H. Daverfeldt and R. Kleiss, Nucl. Phys. **B 253** (1985) 441.

[18] `KORALW` version 1.33 is used:
M. Skrzypek *et al.*, Comp. Phys. Comm. **94** (1996) 216;
M. Skrzypek *et al.*, Phys. Lett. **B 372** (1996) 289.

[19] `EXCALIBUR` version 1.11 is used:
F.A. Berends, R. Pittau and R. Kleiss, Comp. Phys. Comm. **85** (1995) 437.

[20] `NUNUGPV` Monte Carlo:
G. Montagna *et al.*, Nucl. Phys. **B 541** (1999) 31.

[21] `GEANT` Version 3.15 is used:
R. Brun *et al.*, preprint CERN DD/EE/84-1 (1984); revised 1987.
The `GHEISHA` program (H. Fesefeldt, RWTH Aachen Report PITHA 85/02 (1985)) is used to simulate hadronic interactions.

[22] L3 Collab., R. Bizzarri *et al.*, Nucl. Instr. and Meth. **A 317** (1992) 463.

[23] G. D'Agostini, *Proceedings of the Workshop on Confidence Limits*, Geneva, 2000, hep-ex/0002055.

[24] L3 Collab., P. Achard *et al.*, Phys. Lett. **B 572** (2003) 133.

The L3 Collaboration:

P.Achard,[20] O.Adriani,[17] M.Aguilar-Benitez,[25] J.Alcaraz,[25] G.Alemanni,[23] J.Allaby,[18] A.Aloisio,[30] M.G.Alviggi,[30] H.Anderhub,[50] V.P.Andreev,[6,35] F.Anselmo,[8] A.Arefiev,[29] T.Azemoon,[3] T.Aziz,[9] P.Bagnaia,[40] A.Bajo,[25] G.Baksay,[27] L.Baksay,[27] S.V.Baldew,[2] S.Banerjee,[9] Sw.Banerjee,[4] A.Barczyk,[50,48] R.Barillère,[18] P.Bartalini,[23] M.Basile,[8] N.Batalova,[47] R.Battiston,[34] A.Bay,[23] F.Becattini,[17] U.Becker,[13] F.Behner,[50] L.Bellucci,[17] R.Berbeco,[3] J.Berdugo,[25] P.Berges,[13] B.Bertucci,[34] B.L.Betev,[50] M.Biasini,[34] M.Biglietti,[30] A.Biland,[50] J.J.Blaising,[4] S.C.Blyth,[36] G.J.Bobbink,[2] A.Böhm,[1] L.Boldizsar,[12] B.Borgia,[40] S.Bottai,[17] D.Bourilkov,[50] M.Bourquin,[20] S.Braccini,[20] J.G.Branson,[42] F.Brochu,[4] J.D.Burger,[13] W.J.Burger,[34] X.D.Cai,[13] M.Capell,[13] G.Cara Romeo,[8] G.Carlino,[30] A.Cartacci,[17] J.Casaus,[25] F.Cavallari,[40] N.Cavallo,[37] C.Cecchi,[34] J.A.R.Cembranos,[26] M.Cerrada,[25] M.Chamizo,[20] Y.H.Chang,[45] M.Chemarin,[24] A.Chen,[45] G.Chen,[7] G.M.Chen,[7] H.F.Chen,[22] H.S.Chen,[7] G.Chiefari,[30] L.Cifarelli,[41] F.Cindolo,[8] I.Clare,[13] R.Clare,[39] G.Coignet,[4] N.Colino,[25] S.Costantini,[40] B.de la Cruz,[25] S.Cucciarelli,[34] J.A.van Dalen,[32] R.de Asmundis,[30] P.Déglon,[20] J.Debreczeni,[12] A.Degré,[4] K.Dehmelt,[27] K.Deiters,[48] D.della Volpe,[30] E.Delmeire,[20] P.Denes,[38] F.DeNotaristefani,[40] A.De Salvo,[50] M.Diemoz,[40] M.Dierckxsens,[2] C.Dionisi,[40] M.Dittmar,[50] A.Doria,[30] M.T.Dova,[10,♯] D.Duchesneau,[4] M.Duda,[1] B.Echenard,[20] A.Eline,[18] A.El Hage,[1] H.El Mamouni,[24] A.Engler,[36] F.J.Eppling,[13] P.Extermann,[20] M.A.Falagan,[25] S.Falciano,[40] A.Favara,[33] J.Fay,[24] O.Fedin,[35] M.Felcini,[50] T.Ferguson,[36] H.Fesefeldt,[1] E.Fiandrini,[34] J.H.Field,[20] F.Filthaut,[32] P.H.Fisher,[13] W.Fisher,[38] I.Fisk,[42] G.Forconi,[13] K.Freudenreich,[50] C.Furetta,[28] Yu.Galaktionov,[29,13] S.N.Ganguli,[9] P.Garcia-Abia,[25] M.Gataullin,[33] S.Gentile,[40] S.Giagu,[40] Z.F.Gong,[22] G.Grenier,[24] O.Grimm,[50] M.W.Gruenewald,[16] M.Guida,[41] V.K.Gupta,[38] A.Gurtu,[9] L.J.Gutay,[47] D.Haas,[5] D.Hatzifotiadou,[8] T.Hebbeker,[1] A.Hervé,[18] J.Hirschfelder,[36] H.Hofer,[50] M.Hohlmann,[27] G.Holzner,[50] S.R.Hou,[45] Y.Hu,[32] B.N.Jin,[7] L.W.Jones,[3] P.de Jong,[2] I.Josa-Mutuberría,[25] M.Kaur,[14] M.N.Kienzle-Focacci,[20] J.K.Kim,[44] J.Kirkby,[18] W.Kittel,[32] A.Klimentov,[13,29] A.C.König,[32] M.Kopal,[47] V.Koutsenko,[13,29] M.Kräber,[50] R.W.Kraemer,[36] A.Krüger,[49] A.Kunin,[13] P.Ladron de Guevara,[25] I.Laktineh,[24] G.Landi,[17] M.Lebeau,[18] A.Lebedev,[13] P.Lebrun,[24] P.Lecomte,[50] P.Lecoq,[18] P.Le Coultre,[50] J.M.Le Goff,[18] R.Leiste,[49] M.Levtchenko,[28] P.Levtchenko,[35] C.Li,[22] S.Likhoded,[49] C.H.Lin,[45] W.T.Lin,[45] F.L.Linde,[2] L.Lista,[30] Z.A.Liu,[7] W.Lohmann,[49] E.Longo,[40] Y.S.Lu,[7] C.Luci,[40] L.Luminari,[40] W.Lustermann,[50] W.G.Ma,[22] L.Malgeri,[20] A.Malinin,[29] C.Maña,[25] J.Mans,[38] J.P.Martin,[24] F.Marzano,[40] K.Mazumdar,[9] R.R.McNeil,[6] S.Mele,[18,30] L.Merola,[30] M.Meschini,[17] W.J.Metzger,[32] A.Mihul,[11] H.Milcent,[18] G.Mirabelli,[40] J.Mnich,[1] G.B.Mohanty,[9] G.S.Muanza,[24] A.J.M.Muijs,[2] B.Musicar,[42] M.Musy,[40] S.Nagy,[15] S.Natale,[20] M.Napolitano,[30] F.Nessi-Tedaldi,[50] H.Newman,[33] A.Nisati,[40] T.Novak,[32] H.Nowak,[49] R.Ofierzynski,[50] G.Organtini,[40] I.Pal,[47] C.Palomares,[25] P.Paolucci,[30] R.Paramatti,[40] G.Passaleva,[17] S.Patricelli,[30] C.Pattison,[18] T.Paul,[10] M.Pauluzzi,[34] C.Paus,[13] F.Pauss,[50] M.Pedace,[40] S.Pensotti,[28] D.Perret-Gallix,[4] B.Petersen,[32] D.Piccolo,[30] F.Pierella,[8] M.Pioppi,[34] P.A.Piroué,[38] E.Pistolesi,[28] V.Plyaskin,[29] M.Pohl,[20] V.Pojidaev,[17] J.Pothier,[18] D.Prokofiev,[35] J.Quartieri,[41] G.Rahal-Callot,[50] M.A.Rahaman,[9] P.Raics,[15] N.Raja,[9] R.Ramelli,[50] P.G.Rancoita,[28] R.Ranieri,[17] A.Raspereza,[49] P.Razis,[31] D.Ren,[50] M.Rescigno,[40] S.Reucroft,[10] S.Riemann,[49] K.Riles,[3] B.P.Roe,[3] L.Romero,[25] A.Rosca,[49] C.Rosemann,[1] C.Rosenbleck,[1] S.Rosier-Lees,[4] S.Roth,[1] J.A.Rubio,[18] G.Ruggiero,[17] H.Rykaczewski,[50] A.Sakharov,[50] S.Saremi,[6] S.Sarkar,[40] J.Salicio,[18] E.Sanchez,[25] C.Schäfer,[18] V.Schegelsky,[35] H.Schopper,[21] D.J.Schotanus,[32] C.Sciacca,[30] L.Servoli,[34] S.Shevchenko,[33] N.Shivarov,[43] V.Shoutko,[13] E.Shumilov,[29] A.Shvorob,[33] D.Son,[44] C.Souga,[24] P.Spillantini,[17] M.Steuer,[13] D.P.Stickland,[38] B.Stoyanov,[43] A.Straessner,[20] K.Sudhakar,[9] G.Sultanov,[43] L.Z.Sun,[22] S.Sushkov,[1] H.Suter,[50] J.D.Swain,[10] Z.Szillasi,[27,¶] X.W.Tang,[7] P.Tarjan,[15] L.Tauscher,[5] L.Taylor,[10] B.Tellili,[24] D.Teyssier,[24] C.Timmermans,[32] Samuel C.C.Ting,[13] S.M.Ting,[13] S.C.Tonwar,[9] J.Tóth,[12] C.Tully,[38] K.L.Tung,[7] J.Ulbricht,[50] E.Valente,[40] R.T.Van de Walle,[32] R.Vasquez,[47] V.Veszpremi,[27] G.Vesztergombi,[12] I.Vetlitsky,[29] D.Vicinanza,[41] G.Viertel,[50] S.Villa,[39] M.Vivargent,[4] S.Vlachos,[5] I.Vodopianov,[27] H.Vogel,[36] H.Vogt,[49] I.Vorobiev,[36,29] A.A.Vorobyov,[35] M.Wadhwa,[5] Q.Wang[32] X.L.Wang,[22] Z.M.Wang,[22] M.Weber,[18] H.Wilkens,[32] S.Wynhoff,[38] L.Xia,[33] Z.Z.Xu,[22] J.Yamamoto,[3] B.Z.Yang,[22] C.G.Yang,[7] H.J.Yang,[3] M.Yang,[7] S.C.Yeh,[46] An.Zalite,[35] Yu.Zalite,[35] Z.P.Zhang,[22] J.Zhao,[22] G.Y.Zhu,[7] R.Y.Zhu,[33] H.L.Zhuang,[7] A.Zichichi,[8,18,19] B.Zimmermann,[50] M.Zöller.[1]

1 III. Physikalisches Institut, RWTH, D-52056 Aachen, Germany[§]
2 National Institute for High Energy Physics, NIKHEF, and University of Amsterdam, NL-1009 DB Amsterdam, The Netherlands
3 University of Michigan, Ann Arbor, MI 48109, USA
4 Laboratoire d'Annecy-le-Vieux de Physique des Particules, LAPP,IN2P3-CNRS, BP 110, F-74941 Annecy-le-Vieux CEDEX, France
5 Institute of Physics, University of Basel, CH-4056 Basel, Switzerland
6 Louisiana State University, Baton Rouge, LA 70803, USA
7 Institute of High Energy Physics, IHEP, 100039 Beijing, China[△]
8 University of Bologna and INFN-Sezione di Bologna, I-40126 Bologna, Italy
9 Tata Institute of Fundamental Research, Mumbai (Bombay) 400 005, India
10 Northeastern University, Boston, MA 02115, USA
11 Institute of Atomic Physics and University of Bucharest, R-76900 Bucharest, Romania
12 Central Research Institute for Physics of the Hungarian Academy of Sciences, H-1525 Budapest 114, Hungary[‡]
13 Massachusetts Institute of Technology, Cambridge, MA 02139, USA
14 Panjab University, Chandigarh 160 014, India
15 KLTE-ATOMKI, H-4010 Debrecen, Hungary[¶]
16 Department of Experimental Physics, University College Dublin, Belfield, Dublin 4, Ireland
17 INFN Sezione di Firenze and University of Florence, I-50125 Florence, Italy
18 European Laboratory for Particle Physics, CERN, CH-1211 Geneva 23, Switzerland
19 World Laboratory, FBLJA Project, CH-1211 Geneva 23, Switzerland
20 University of Geneva, CH-1211 Geneva 4, Switzerland
21 University of Hamburg, D-22761 Hamburg, Germany
22 Chinese University of Science and Technology, USTC, Hefei, Anhui 230 029, China[△]
23 University of Lausanne, CH-1015 Lausanne, Switzerland
24 Institut de Physique Nucléaire de Lyon, IN2P3-CNRS,Université Claude Bernard, F-69622 Villeurbanne, France
25 Centro de Investigaciones Energéticas, Medioambientales y Tecnológicas, CIEMAT, E-28040 Madrid, Spain♭
26 Universidad Complutense de Madrid, E-28040 Madrid, Spain
27 Florida Institute of Technology, Melbourne, FL 32901, USA
28 INFN-Sezione di Milano, I-20133 Milan, Italy
29 Institute of Theoretical and Experimental Physics, ITEP, Moscow, Russia
30 INFN-Sezione di Napoli and University of Naples, I-80125 Naples, Italy
31 Department of Physics, University of Cyprus, Nicosia, Cyprus
32 University of Nijmegen and NIKHEF, NL-6525 ED Nijmegen, The Netherlands
33 California Institute of Technology, Pasadena, CA 91125, USA
34 INFN-Sezione di Perugia and Università Degli Studi di Perugia, I-06100 Perugia, Italy
35 Nuclear Physics Institute, St. Petersburg, Russia
36 Carnegie Mellon University, Pittsburgh, PA 15213, USA
37 INFN-Sezione di Napoli and University of Potenza, I-85100 Potenza, Italy
38 Princeton University, Princeton, NJ 08544, USA
39 University of Californa, Riverside, CA 92521, USA
40 INFN-Sezione di Roma and University of Rome, "La Sapienza", I-00185 Rome, Italy
41 University and INFN, Salerno, I-84100 Salerno, Italy
42 University of California, San Diego, CA 92093, USA
43 Bulgarian Academy of Sciences, Central Lab. of Mechatronics and Instrumentation, BU-1113 Sofia, Bulgaria
44 The Center for High Energy Physics, Kyungpook National University, 702-701 Taegu, Republic of Korea
45 National Central University, Chung-Li, Taiwan, China
46 Department of Physics, National Tsing Hua University, Taiwan, China
47 Purdue University, West Lafayette, IN 47907, USA
48 Paul Scherrer Institut, PSI, CH-5232 Villigen, Switzerland
49 DESY, D-15738 Zeuthen, Germany
50 Eidgenössische Technische Hochschule, ETH Zürich, CH-8093 Zürich, Switzerland
§ Supported by the German Bundesministerium für Bildung, Wissenschaft, Forschung und Technologie.
‡ Supported by the Hungarian OTKA fund under contract numbers T019181, F023259 and T037350.
¶ Also supported by the Hungarian OTKA fund under contract number T026178.
♭ Supported also by the Comisión Interministerial de Ciencia y Tecnología.
♯ Also supported by CONICET and Universidad Nacional de La Plata, CC 67, 1900 La Plata, Argentina.
△ Supported by the National Natural Science Foundation of China.

$\sqrt{s}$ (GeV)	$\mathcal{L}$ (pb^{-1})	N_D	N_B	N_S
188.6	176.8	129	126.3	20.9
191.6	29.8	22	23.1	4.1
195.5	84.1	63	65.7	12.8
199.5	83.3	59	63.7	18.0
201.7	37.2	30	28.9	8.8
202.5−205.5	79.0	51	59.9	20.5
205.5−209.2	139.0	101	102.2	37.9
Total	629.2	455	469.8	123.0

Table 1: Luminosity, number of selected data events, N_D, and expected Standard Model background events, N_B, as a function of $\sqrt{s}$ in the search for the $\mathrm{e^+e^-} \rightarrow \tilde{\pi}\tilde{\pi}\mathrm{Z} \rightarrow \tilde{\pi}\tilde{\pi}\mathrm{q\bar{q}}$ process. The expected number of signal events, N_S, is also given for $M = 0$ and $f = 40$ GeV.

		High p_t			Low p_t		
$\sqrt{s}$ (GeV)	$\mathcal{L}$ (pb^{-1})	N_D	N_B	N_S	N_D	N_B	N_S
188.6	176.0	249	254.7	71.0	156	152.9	16.6
191.6	29.5	37	40.2	13.0	32	28.2	3.5
195.5	83.9	123	110.1	42.9	73	80.1	11.5
199.5	81.3	114	102.6	47.2	74	77.0	13.0
201.7	34.8	53	43.9	21.8	35	32.7	6.0
202.5−205.5	74.8	103	90.4	52.3	71	70.6	15.1
205.5−207.2	130.2	151	158.9	96.5	93	105.9	27.7
207.2−209.2	8.6	8	10.4	6.7	9	7.0	1.9
Total	619.1	838	811.2	351.4	543	554.4	95.3

Table 2: Luminosity, number of selected data events, N_D, and expected Standard Model background events, N_B, as a function of $\sqrt{s}$ for the high-p_t and the low-p_t single-photon selections. Expectations, N_S, for branon production through the $\mathrm{e^+e^-} \rightarrow \tilde{\pi}\tilde{\pi}\gamma$ process are also given for $M = 0$ and $f = 150$ GeV.

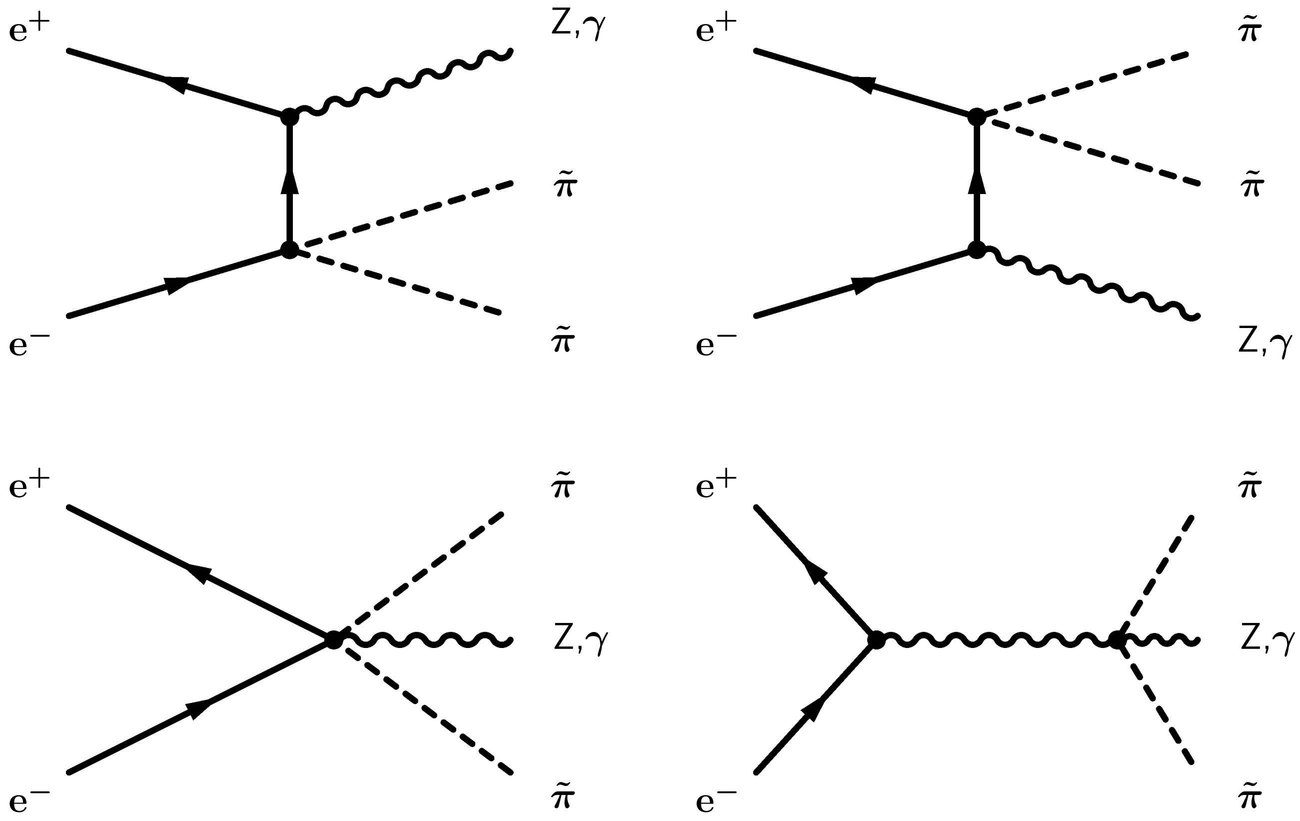

Figure 1: Feynman diagrams contributing to the branon production process: $e^+e^- \to \tilde{\pi}\tilde{\pi}V_0$, where V_0 denotes a photon or a Z boson.

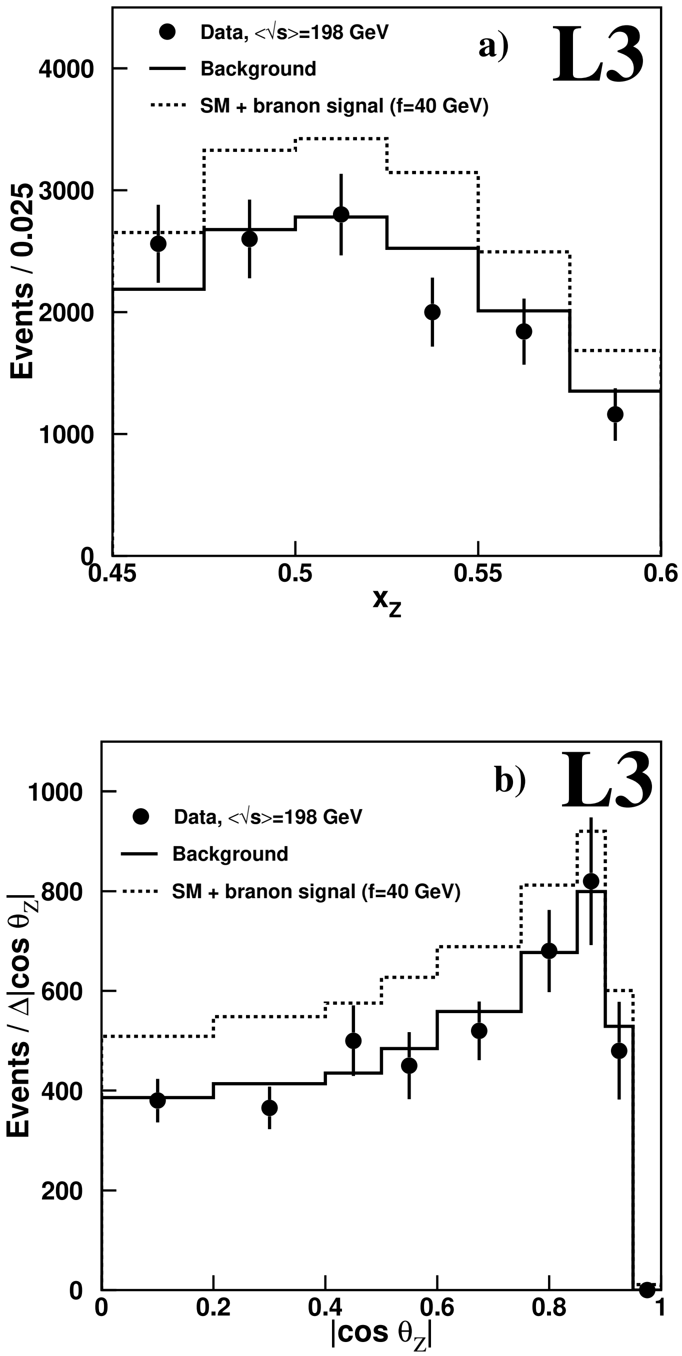

Figure 2: Distributions for events selected in the $e^+e^- \to \tilde{\pi}\tilde{\pi}Z \to \tilde{\pi}\tilde{\pi}q\overline{q}$ search: a) the reduced energy of the Z boson, $x_Z = E_Z/\sqrt{s}$, and b) the absolute value of the cosine of its polar angle, θ_Z. The points represent the data, the solid histogram is the expectation from Standard Model processes and the dashed histogram is an example of the expectations in the presence of an additional signal due to branon production with $M = 0$ and $f = 40$ GeV.

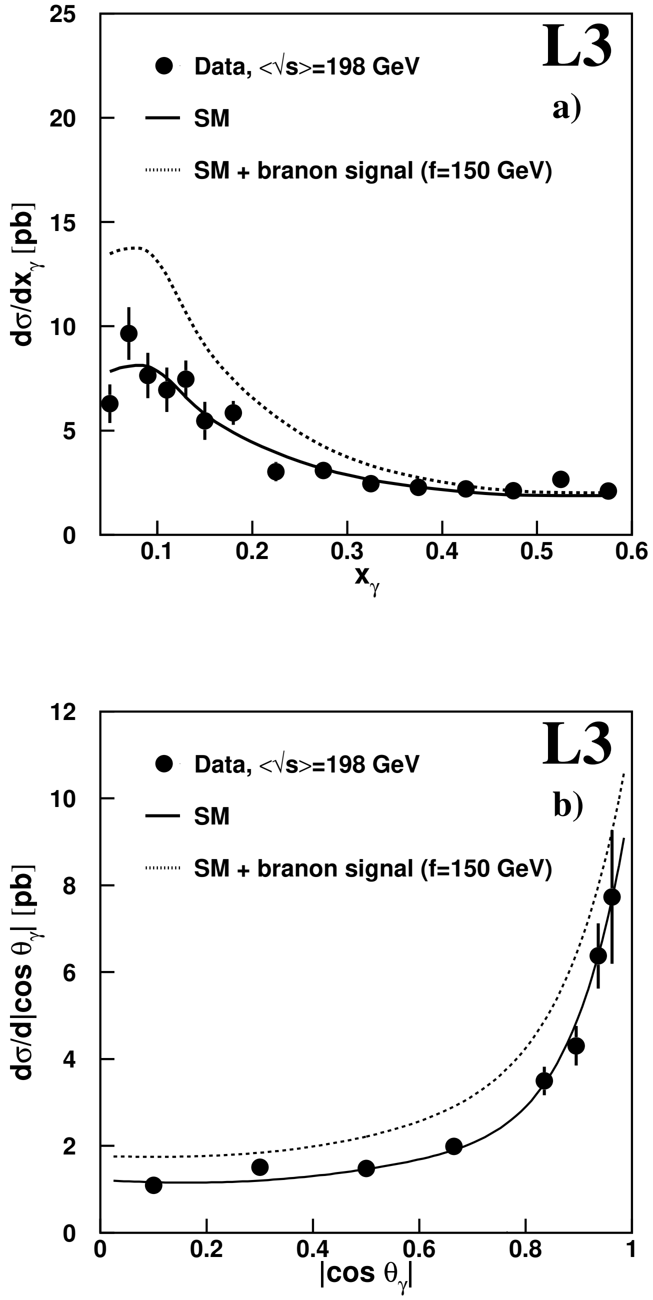

Figure 3: Measured differential cross sections for the $\mathrm{e^+e^-} \rightarrow \nu\bar{\nu}\gamma(\gamma)$ process as a function of a) $x_\gamma = E_\gamma/E_{beam}$, the fraction of the beam energy carried by the photon and b) the absolute value of the cosine of its polar angle, θ_γ. Data selected by the high-p_t selection at $0.04E_{beam} < p_t < 0.6E_{beam}$ are shown. They are integrated over the fiducial region $|\cos\theta_\gamma| < 0.97$. The points represent the data, the solid curves are the Standard Model predictions and the dashed curves show the expectations in the presence of an additional signal due to branon production with $M = 0$ and $f = 150$ GeV.

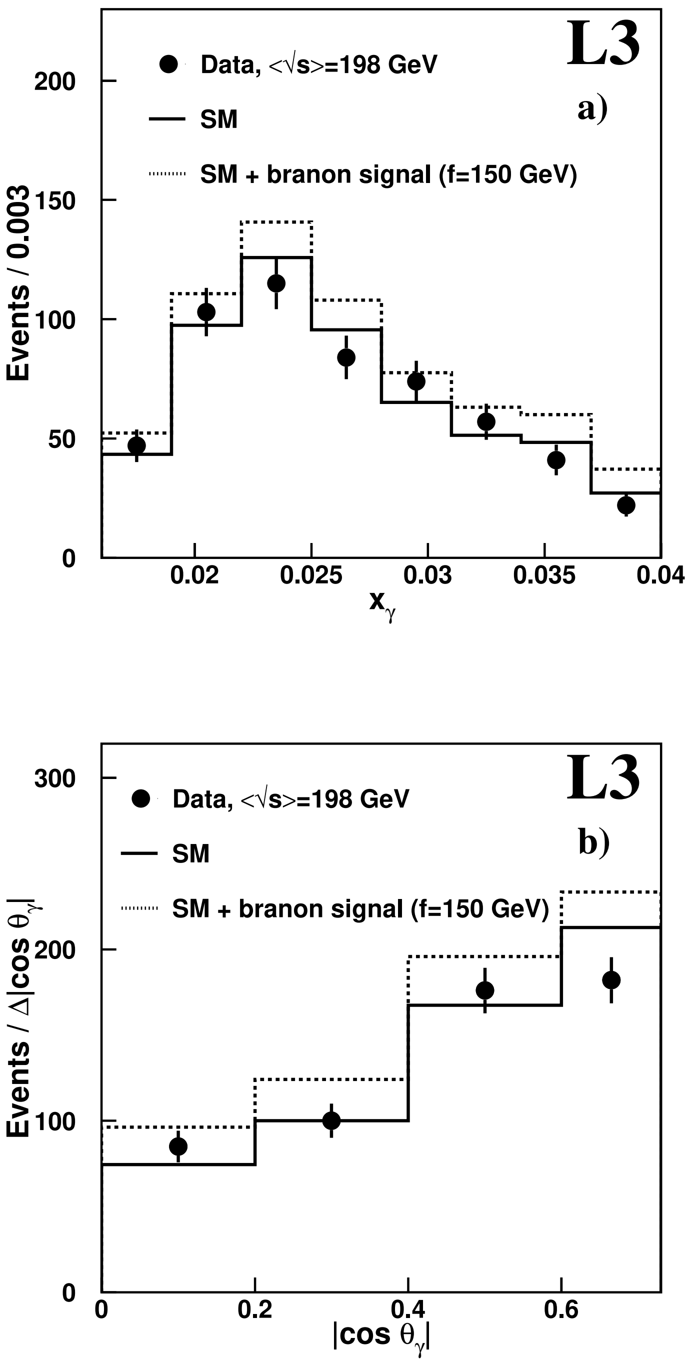

Figure 4: Distributions for events selected by the low-p_t selection at $0.016E_{beam} < p_t < 0.04E_{beam}$ in the $\mathrm{e}^+\mathrm{e}^- \rightarrow \tilde{\pi}\tilde{\pi}\gamma$ search: a) the fraction of the beam energy carried by the photon, $x_\gamma = E_\gamma/E_{beam}$ and b) the absolute value of the cosine of its polar angle, θ_γ. The points represent the data, the solid histogram is the expectation from Standard Model processes and the dashed histogram is an example of the expectations in the presence of an additional signal due to branon production with $M = 0$ and $f = 150$ GeV.

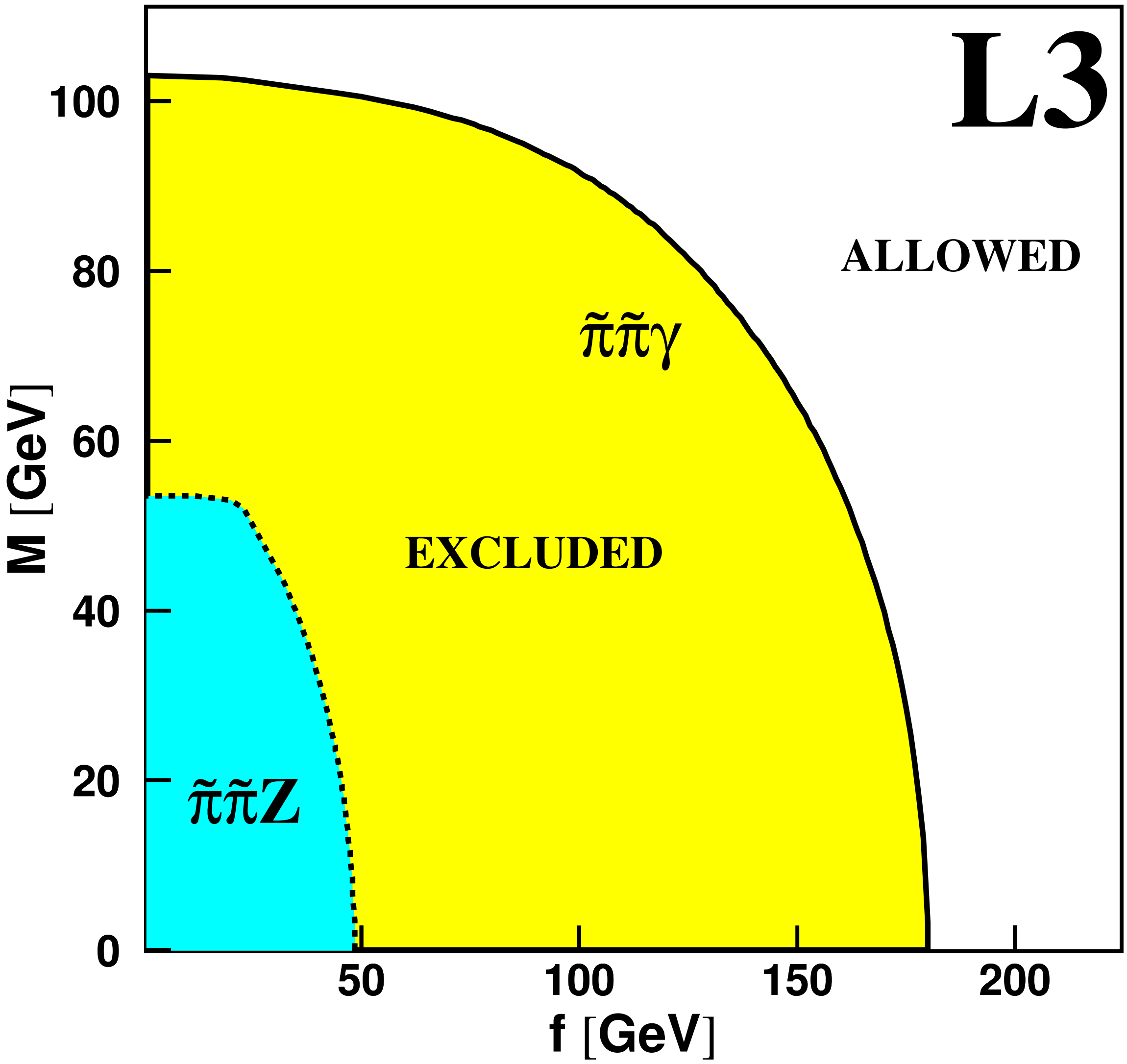

Figure 5: Two-dimensional regions in the (f, M) plane excluded by the searches for branons produced in the $e^+e^- \to \tilde{\pi}\tilde{\pi}Z$ and $e^+e^- \to \tilde{\pi}\tilde{\pi}\gamma$ processes. For very elastic branes, $f \to 0$, branon masses below 103 GeV are excluded at 95% confidence level. For massless branons, brane tensions below 180 GeV are excluded.